STUDY OF FLUID FLOWS USING SMOOTHED PARTICLE HYDRODYNAMICS: THE MODIFIED PRESSURE CONCEPT APPLIED TO QUIESCENT FLUID AND DAM BREAKING

Carlos Alberto Dutra Fraga Filho[1]

Julio Tomás Aquije Chacaltana[2]

cadff1@gmail.com

juliotac@gmail.com

1 – Federal Institute of Espírito Santo – Mechanical Coordination – Av. Vitória, 1729 – 29040-620 – Jucutuquara – Vitória – ES – Brazil

2 – Federal University of Espírito Santo – Environmental Engineering Department – Laboratory of Simulation of Free Surface Flows (LABESUL) – Av. Fernando Ferrari, 514 – 29075-910 – Goiabeiras – Vitória – ES – Brazil

Abstract. *Smoothed Particle Hydrodynamics (SPH) is one of the Lagrangian methods used in fluid mechanics to address complex fluid flow with a free surface or interfaces, producing results consistent with those obtained by analytical and experimental techniques. The focus of this work is to show that when the modified pressure concept for quiescent and incompressible fluid is applied, the numerical solution of the Navier-Stokes equations by the SPH method produces better results compared with analytical ones. A code in Fortran language is written to solve the system of algebraic equations. The numerical model, SPH, is applied to analyse the particle movement of quiescent fluid in a reservoir and the particle fluid flow movement when a dam break occurs. In the case of fluid at rest, results obtained using SPH show that particles do not remain in their initial positions and that their movements increase as time progresses. Contrary to literature reports, the modified pressure concept used in this work produces results similar to those provided by analytical solution. In the dam break case, an artificial viscosity was used to avoid instabilities in particle movement. The inconsistency found in the interpolated value of the function near the boundary was corrected by introducing a correction factor. To prevent fluid particles from crossing the rigid boundary, the concept of reflection of particles with a coefficient of restitution of kinetic energy was used. In this case the numerical results agree with those obtained in laboratory experiments, with a maximum difference of 17.86%.*

Keywords: *SPH method, fluid at rest, modified pressure, coefficient of restitution of kinetic energy, dam breaking*

1 INTRODUCTION

Smoothed Particle Hydrodynamics (SPH) is one of the Lagrangian methods that have been increasingly used in fluid flow problems involved with free surfaces or interfaces. This Lagrangian method was originally developed by Lucy (1977) and Gingold and Monaghan (1977) for modelling astrophysical phenomena. SPH does not use meshes, and it easily discretizes complex geometries, more easily refines the domain, and easily captures the free surfaces and their topological changes. Among the disadvantages of this method, an appropriate implementation of boundary conditions, the inconsistencies found in physical quantities interpolated for particles close to the boundaries, and agglomeration of particles in certain regions of the domain can be cited.

The solution for an incompressible and isothermal fluid at rest in a reservoir is well known. Each fluid particle, fixed in space without movement, must satisfy the equations that represent the physical laws of mass and momentum. This hydrostatic problem was treated by Vorobyev (2013) using SPH and employing various formulations for the viscous term. The results presented by Vorobyev showed fluctuations in the positions occupied by the particles that progress in time.

Goffin et al. (2014) employed the SPH method to study the particle movement of a fluid in a tank for situations when the tank is filled with water and both are at rest and when the tank is in rotation and during dam breaking in a dry bed. The numerical results presented showed undesirable effects. In the first case, the particles oscillate and change their spatial positions within the reservoir over time. For the tank in rotation, the influence of sound speed magnitude on fluid compressibility was observed. In the breaking dam case, an agglomeration of particles was found to occur on the wall tank, which was reduced by using a symmetry condition.

The clustering of particles was handled by Korzilius et al. (2014), who proposed two solutions to the problem that happens in certain portions of the domain and is caused by the decreasing kernel gradient values in small distances between particles. The first method employs a convex kernel with non-zero gradient at the origin, and the second one is based on the implementation of collisions between particles. Results were presented for the problem of a tank filled with water at rest. When the first proposed solution was used, despite the reduction of the influence of the particles of the free surface and contour (virtual particles) in the numerical calculation of the pressure gradient, errors were also found in the SPH approximations, with fluctuations in the values of gradients around the analytical solution. The fluctuations became smaller over time and converged to a steady state system which was, however, divergent from the correct state. For the same length of smoothing, the results obtained with the convex kernel were worse than those obtained with a regular Wendland kernel. However, by increasing the length of smoothing, the errors became smaller. When collisions between particles were implemented, it was found that there was no influence on the pressures encountered.

Fourtakas et al. (2015) also studied a reservoir filled with a fluid at rest and dam break. They proposed a new method for the contour treatment using virtual particles. An improvement was achieved for the consistencies of the zeroth and first orders. Although the results for the first case showed an improvement over the conventional techniques, a change in the positions of fluid particles inside the reservoir was still noticed. For the dam break, there was an agreement with the experimental results, and the smallest errors were achieved when the distance between the particles decreased.

Many researchers have employed the SPH technique to obtain the numerical solution of a fluid at rest. Until now, the results have not been not fully satisfactory compared with theoretical ones reported in the literature. In this paper, to solve the hydrostatic problem with SPH, the modified pressure concept (Batchelor, 2000) was used. This produces numerical results in agreement with those found by the analytical solution. The dynamic case is also treated by using traditional SPH modelling for the dam break. In this case, the boundary conditions were fixed geometric planes at the solid boundaries and a coefficient of restitution of kinetic energy was used for treatment of the collisions between fluid particles against the rigid boundaries. For this study, the SPH results were validated through the comparison with experiments.

This paper is organized in sections as follows. In Section 2 the mathematical modelling and modified pressure concept are presented. The numerical treatment of the set of equations by the SPH Lagrangian method is discussed in Section 3. The results and discussion of the results are in Section 4. Finally, the conclusion of this study is presented in Section 5.

2 MATHEMATICAL MODELLING

The mathematical modelling of a fluid flow and energy transport of a viscous and incompressible fluid is performed by the mass, momentum, and energy laws, which are expressed by the conservation equations: Eqs. (1), (2), and (3), respectively.

$$\frac{D\rho}{Dt} + \rho\nabla.\vec{\mathrm{v}} = 0 \tag{1}$$

where ρ is the density, t is the time, ∇ is the mathematical nabla operator, and $\vec{\mathrm{v}}$ is the velocity.

$$\frac{D\vec{\mathrm{v}}}{Dt} = \frac{1}{\rho}\left(-\nabla P + \mu\nabla^2\vec{\mathrm{v}} + \rho\,\vec{g}\right) \tag{2}$$

where P is the absolute pressure, μ is the dynamic viscosity, and $\vec{g}$ is the gravitational acceleration.

$$\frac{De}{Dt} = \frac{1}{\rho}\left(-P(\nabla.\vec{\mathrm{v}}) + \varepsilon_{\mathrm{v}} + \nabla\cdot(k\nabla T) + \dot{q}\right) \tag{3}$$

where e is the specific internal energy, ε_{v} is the rate of energy dissipation per unit volume, k is the thermal conductivity, T is the absolute temperature, and $\dot{q}$ is the rate of heating provided by the source per unit volume.

2.1 Equation of state for dynamic pressure

The dynamic pressure of the fluid is calculated by Equation (4), known as the Tait equation, suggested in Batchelor (2000):

$$P_{\mathrm{dyn}} = B\left[\left(\frac{\rho}{\rho_o}\right)^{\gamma} - 1\right] \tag{4}$$

where P_{dyn} is the dynamic pressure, B is the term associated with fluctuations in the fluid density, ρ_o is the fluid density at rest, and $\gamma = 7$.

For the Tait equation to be applied in predicting the dynamic pressure, it must be ensured that the Mach number, defined in Eq. (5), is not greater than 0.1.

$$Ma = \frac{\mathrm{v}}{\mathrm{c}_0} < 0{,}1 \tag{5}$$

where Ma is the Mach number, v is the magnitude of flow velocity, and c_0 is the magnitude of sound velocity in the fluid.

2.2 Modified Pressure

The modified pressure concept for a uniform, viscous, and incompressible fluid was presented by Batchelor (2000). It is defined as the remaining part of the pressure that exceeds the amount sufficient to balance the gravitational force, causing the fluid movement. This concept is presented mathematically by Eq. (6):

$$P_{\mathrm{mod}} = \left(P - P_0\right) - \rho g (H - \mathrm{y}) \tag{6}$$

where P_{mod} is the modified pressure, P_0 is the reference pressure, H is the fluid level and y is the ordinate of the position occupied by the fluid (when referential is fixed at bottom).

The use of the modified pressure changes the form of the momentum balance equation, as shown in Eq. (7).

$$\frac{D\vec{\mathrm{v}}}{Dt} = -\frac{\nabla P_{\mathrm{mod}}}{\rho} + \upsilon \nabla^2 \vec{\mathrm{v}} \tag{7}$$

where υ is the kinematic viscosity.

This concept can be applied to cases of hydrostatic or fluid dynamics. In hydrostatic cases, the modified pressure is zero. In the dynamic cases, it is the difference between the dynamic pressure and the term $\rho g (H - \mathrm{y})$, where g is the magnitude of the gravitational acceleration.

In this work, the concept of the modified pressure was implemented to study an incompressible, viscous, and isothermal fluid at rest inside a reservoir.

2.3 Specific internal energy

The specific heat at constant volume (c_{v}) is defined for an incompressible fluid flow.

$$c_{\mathrm{v}} = \left(\frac{De}{DT}\right)_{\mathrm{v\ constant}} \tag{8}$$

In the case of an isothermal fluid, it has zero value. Consequently, the mathematical modelling of a viscous, incompressible, and isothermal fluid is performed only by the mass conservation and momentum balance equations.

3 NUMERICAL MODELLING

SPH is based on the mathematical identity, valid for a defined and continuous function, according to Eq. (9):

$$f(X) = \int f(X')\delta(X - X')dX' \tag{9}$$

where $f(X)$ is the value of the scalar function at the fixed point X, $f(X')$ is the value of the scalar function at the variable point X', $\delta(X - X')$ is the Dirac delta function, and dX' is the infinitesimal volume element.

By replacing the Dirac delta function by a kernel, the approximation to the function in position is obtained, resulting in Eq. (10):

$$\langle f(X)\rangle = \int f(X')W(X - X',h)dX' \tag{10}$$

where $\langle f(X)\rangle$ is the approximated value of the scalar function at the fixed point X, $W(X - X',h)$ is the kernel, and h is the support radius.

The essence of the SPH method is to discretize the domain into a finite number of particles which get the physical quantities of interest from weighted interpolations of the quantities in the neighboring particles. Only those particles that are within the domain of influence (at a maximum distance kh from the fixed particle considered) will contribute to the behaviour of the fixed particle. Figure 1 shows a graphical representation of particles within the domain of influence.

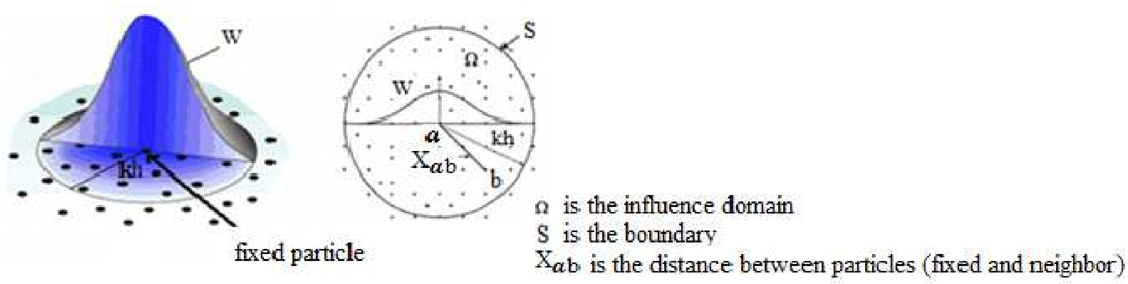

Figure 1. Graphical representation of the domain of influence. The fixed particle a has as neighbors all particles within the domain of influence (particles b), $\mathbf{k}$ is a scale factor which depends of used kernel.

Success in the approximations depends on having a sufficient number of particles within the domain of influence. Numerical tests have been conducted and have shown that, in a two-dimensional case, it is necessary to have at least 21 particles within the domain of influence to assure the properties of the kernel and its gradient (anti-symmetry and non-normalization) and, consequently, the accuracy of results obtained in interpolations (Fraga Filho, 2014). Increasing the number of neighboring particles further does not significantly alter the numerical results, but does however affect the time spent in the simulation. Figure 2 shows a 2D cell whose domain of influence has 21 particles inside.

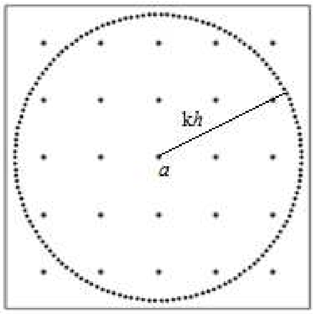

Figure 2. A 2D cell with 21 particles within the domain of influence.

By discretization of the domain by particles, the following relation is obtained:

$$dX' = \frac{dm'}{\rho'} \tag{11}$$

where dm' is the mass of the infinitesimal volume element of the fluid and ρ' is the fluid density.

By combining Eqs. (10) and (11), an SPH approximation for a scalar property of the fluid is obtained according to Eq. (12):

$$f_a = \sum_{b=1}^{n} m_b \frac{f_b}{\rho_b} W(X_a - X_b, h) \tag{12}$$

where f_a is the approximate value of the function in the fixed particle's position, f_b is the approximate value of the function in the neighboring particle position, X_a is the fixed particle's position, X_b is the neighboring particle's position, m_b and ρ_b are the mass and density of the neighboring particle, respectively, and n is the number of neighboring particles.

The SPH approximations for the divergent, gradient, and Laplacian of a function are presented in Eqs. (13) to (15).

$$\nabla . f_a = \frac{1}{\rho_a} \sum_{b=1}^{n} m_b (f_b - f_a) . \nabla W(X_a - X_b, h) \tag{13}$$

$$\nabla f_a = -\rho_a \sum_{b=1}^{n} m_b \left(\frac{f_a}{\rho_a^2} + \frac{f_b}{\rho_b^2} \right) \nabla W(X_a - X_b, h) \tag{14}$$

$$\nabla^2 f_a = 2 \sum_{b=1}^{n} \frac{m_b}{\rho_b} (f_a - f_b) \frac{X_a - X_b}{|X_a - X_b|^2} . \nabla W(X_a - X_b, h) \tag{15}$$

where ρ_a is the reference particle density, which is held fixed during the interpolation calculation.

Deductions for the approximations presented above can be found in Monaghan (1992) and Fraga Filho (2014).

In the SPH method, different kernels can be used for distribution of the interpolation weights. They have the properties of smoothness, positivity, symmetry, convergence, decay, compact support, and normalization within the domain of influence (Liu and Liu, 2003; Kelager, 2006).

The cubic spline kernel proposed by Liu and Liu (2003) for a 2D domain was used in this work, as presented in Eq. (16). This smoothing function and its derivatives exhibit a desirable mathematical behaviour for the representation of the physical properties.

$$W(X - X',h) \quad = \quad \frac{15}{7\pi h^2} \begin{cases} \dfrac{2}{3} - q^2 + \dfrac{1}{2}q^3, \quad if \quad 0 \le q \le 1 \quad , \\[2ex] \dfrac{1}{6}\left(2 - q^3\right), \qquad if \qquad \le q \le 2 \quad , \\[2ex] 0, \quad in \quad the \quad other \quad case. \end{cases} \tag{16}$$

where $q = \dfrac{\left|X - X'\right|}{h}$.

Other kernels can be employed in the SPH method, such as the quartic proposed by Lucy (1977), the quintic presented by Gomez-Gesteira et al. (2010), the quintic spline proposed by Morris (1997), and the new quartic presented by Liu and Liu (2003), among others.

3.1 Errors in the SPH approximations

The approximations to a function and its derivatives taken by the SPH method have errors. This subject will be discussed below.

Applying the expansion of the Taylor series for the function $f\left(X\right)$, which is differentiable in the domain around the fixed point X :

$$\left\langle f(X)\right\rangle = \int f(X')W(X - X',h)dX' + f'(X)\int\left(X - X'\right)W(X - X',h)dX' + \mathrm{Re}(h^2) \tag{17}$$

where $f'(X)$ is the derivative of the function and $\mathrm{Re}(h^2)$ is the residue of the second order .

Due to kernel symmetry, Eq. (17) results in:

$$\left\langle f(X)\right\rangle = \int f(X')W(X - X',h)dX' + \mathrm{Re}(h^2) \tag{18}$$

From the analysis of Eq. (18), it is seen that the approximation to the function value has a second-order error. Similarly, the approximations for derivatives of the first and second orders also have errors.

3.2 SPH approximations for the mass conservation and momentum balance equations

From the approximations taken to the divergent, gradient, and Laplacian of a function, the SPH expressions for mass conservation and momentum balance equations, Eqs. (19) and (20), are obtained.

$$\frac{D\rho_a}{Dt} = \frac{1}{\rho_a}\sum_{b=1}^{n} m_b (\vec{v}_b - \vec{v}_a).\nabla W(X_a - X_b, h) \tag{19}$$

where $\vec{v}_a$ is the fixed particle velocity and $\vec{v}_b$ is the neighboring particle velocity.

$$\frac{D\vec{v}_a}{Dt} = -\sum_{b=1}^{n} m_b \left(\frac{P_a}{\rho_a^2} + \frac{P_b}{\rho_b^2}\right)\nabla W(X_a - X_b, h) + 2\upsilon_a \sum_{b=1}^{n} \frac{m_b}{\rho_b}(\vec{v}_a - \vec{v}_b)\Delta X.\nabla W(X_a - X_b, h) + \rho_a \vec{g} \tag{20}$$

where:

$$\Delta X = \frac{X_a - X_b}{\left|X_a - X_b\right|^2},$$

P_a is the absolute pressure on the fixed particle,

P_b is the absolute pressure on the neighboring particle,

υ_a is the fixed particle kinematic viscosity.

By application of the modified pressure concept, the momentum balance equation will be written as follows:

$$\frac{D\vec{v}_a}{Dt} = -\sum_{b=1}^{n} m_b \left(\frac{P_{\mathrm{mod}(a)}}{\rho_a^2} + \frac{P_{\mathrm{mod}(b)}}{\rho_b^2}\right)\nabla W(X_a - X_b, h) + 2\upsilon_a \sum_{b=1}^{n} \frac{m_b}{\rho_b}(\vec{v}_a - \vec{v}_b)\Delta X.\nabla W(X_a - X_b, h) \tag{21}$$

where $P_{\mathrm{mod}(a)}$ and $P_{\mathrm{mod}(b)}$ are the modified pressures on the fixed particle and the neighboring particle, respectively.

3.3 Variable Smoothing Length

The length of the domain of influence is very important in the SPH method. It influences the efficiency of the calculations and the accuracy of the solutions. If the length of the domain of influence is too small or too large, the results will not be consistent with the studied physical problem.

In the simulation of problems where there are shocks or impacts with sudden local variation of density, it is necessary to vary the support radius, so that the number of neighboring particles is maintained around a constant value. The need to apply support radius compensation occurs, for example, in the simulation of dam breaking. In this work the following form correction proposed by Liu and Liu was used (2003):

$$\frac{Dh}{Dt} = -\frac{1}{n_d}\frac{h}{\rho}\frac{D\rho}{Dt} \tag{22}$$

where n_d is the number of domain dimensions.

3.4 Artificial Viscosity

The transformation of kinetic energy into heat takes place in problems involving mainly shock waves and needs to be measured, which does not happen when Eqs. (20) to (22) are employed. That energy transformation can be represented as a form of viscous dissipation. Its application in the simulations aims to avoid numerical instabilities and the interpenetration between particles. The formulation used in the modelling of artificial viscosity is shown in Eq. (23), as presented by Liu and Liu (2003).

$$\pi_{ab} = \begin{cases} \dfrac{-\alpha_\pi \chi_{ab} c_{ab} + \beta_\pi \chi_{ab}{}^2}{\rho_{ab}}, & \left(\vec{\mathrm{v}}_a - \vec{\mathrm{v}}_b\right).\left(X_a - X_b\right) < 0, \\ 0, & \left(\vec{\mathrm{v}}_a - \vec{\mathrm{v}}_b\right).\left(X_a - X_b\right) \geq 0. \end{cases} \tag{23}$$

$$\chi_{ab} = \frac{h_{ab}\left(\vec{\mathrm{v}}_a - \vec{\mathrm{v}}_b\right).\left(X_a - X_b\right)}{\left|X_a - X_b\right|^2 + 0,01\varphi^2}, \quad c_{ab} = \frac{c_a + c_b}{2} \quad , \quad \rho_{ab} = \frac{\rho_a + \rho_b}{2} \quad , \quad h_{ab} = \frac{h_a + h_b}{2}.$$

where:

π_{ab} is the artificial viscosity,

α_π and β_π are coefficients used in the calculation of artificial viscosity,

c_a and c_b are the velocities of sound in the fixed and neighboring particles, respectively,

h_a and h_b are the support radii of the fixed and neighboring particles, respectively,

φ^2 is a factor that prevents numerical differences when two particles approach one another.

In the above equations, the factor is set to $0.01\,h_{ab}{}^2$.

The term related to artificial viscosity is added to the terms of pressure in the SPH approximations for the momentum balance and energy conservation equations (Fraga Filho, 2014).

3.5 Consistency

According to the equivalence theorem of Lax-Richtmeyer, it is known that if a numerical model is stable, the convergence of the solution to the well-posed problem will be determined by the consistency of the approximation function.

The consistencies of the zeroth and first orders are guaranteed if Eqs. (24) are satisfied.

$$\begin{cases} M_0 = \int W(X - X', h) dX' = 1, \\ M_1 = \int \left(X - X'\right) W(X - X', h) dX' = 0. \end{cases} \tag{24}$$

where M_0 and M_1 are the moments of the zeroth and first orders, respectively.

The discrete counterparts of the constant and linear consistency conditions presented in Eqs. (25) and (26):

$$\sum_{b=1}^{n} W(X_a - X_b, h) \frac{m_b}{\rho_b} = 1 \tag{25}$$

$$\sum_{b=1}^{n} \left(X_a - X_b\right) W(X_a - X_b, h) \frac{m_b}{\rho_b} = 0 \tag{26}$$

In the SPH method, the consistency depends not only on the function approximation employed but also on the domain of influence, the number of particles, and their distribution within the domain. If the domain of influence is continuous and complete, there is a uniform distribution of particles inside it, and the support radius has been properly defined, the conditions for the consistencies of zeroth and first orders are met due to the properties of normalization and symmetry of the kernel. The influence of the support radius in the approximations obtained by SPH therefore needs to be properly analysed (Liu and Liu, 2010).

When there is an imbalance of particles within the domain of influence (with the existence of more dense regions), the left side of Eq. (25) is less than 1 and the left side of Eq. (26) is not null. The same occurs when there is truncation of the domain of influence, a situation shown in Fig. 3. This phenomenon is known as particle inconsistency.

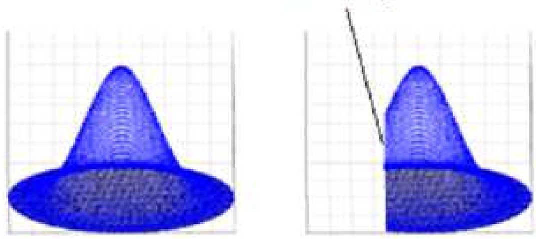

(a) (b)

Figure 3. Domain of influence: (a) complete and (b) incomplete or truncated. It is possible see that the kernel is not defined in a whole domain.

Chen et al. (1999) proposed the application of the Corrected Smoothed Particle Method (CSPM) with the aim of correcting the particle inconsistency. The density is corrected by using the expression given in Eq. (27):

$$\rho_a^* = \frac{\sum_{b=1}^{n} m_b W(X_a - X_b, h)}{\sum_{b=1}^{n} W(X_a - X_b, h)\dfrac{m_b}{\rho_b}} \tag{27}$$

where ρ_a^* is the corrected density of the particle.

The Cartesian components of the pressure gradient in a 2D domain are corrected by using the set of Eqs. (28):

$$\begin{cases} \left(\dfrac{1}{\rho}\dfrac{\partial P}{\partial \mathrm{x}}\right)_a^* = \dfrac{\left(\dfrac{1}{\rho}\dfrac{\partial P}{\partial \mathrm{x}}\right)_a}{\sum_{b=1}^{n} \dfrac{\partial W(X_a - X_b, h)}{\partial \mathrm{x}}(\mathrm{x}_b - \mathrm{x}_a)\dfrac{m_b}{\rho_b}}, \\[2em] \left(\dfrac{1}{\rho}\dfrac{\partial P}{\partial \mathrm{y}}\right)_a^* = \dfrac{\left(\dfrac{1}{\rho}\dfrac{\partial P}{\partial \mathrm{y}}\right)_a}{\sum_{b=1}^{n} \dfrac{\partial W(X_a - X_b, h)}{\partial \mathrm{y}}(\mathrm{y}_b - \mathrm{y}_a)\dfrac{m_b}{\rho_b}}. \end{cases} \tag{28}$$

where:

$\left(\frac{1}{\rho}\frac{\partial P}{\partial \mathrm{x}}\right)^{*}_{a}$ and $\left(\frac{1}{\rho}\frac{\partial P}{\partial \mathrm{y}}\right)^{*}_{a}$ are the components of the kernel gradient, corrected by the CSPM method, per unit mass in the x and y directions, respectively,

x_a is the fixed particle abscissa,

x_b is the neighboring particle abscissa,

y_a is the fixed particle ordinate,

y_b is the neighboring particle ordinate.

3.6 Boundary conditions

Boundary treatment is one of the difficulties presented by the SPH method. Overall, the boundary conditions applied are classified as geometric, repulsive, dynamic, or semi-analytical. Due to the importance and direct influence of the boundaries in obtaining consistent results, this subsection is reserved for the presentation of different boundary treatment methods in the SPH method.

Geometric reflection treatment is the study of the collisions of the particles against the fixed walls of the contours (considering well-defined planes). Figure 4 shows the starting position (C_0) and final position (C_f) of the centre of mass of a particle, after successive collisions with two planes (A and B) occurring in a numerical iteration (Nobrega, 2007). The point C_1 is the final position that would be reached by the centre of mass of the particle if there were no planes delimiting the domain. In the geometric reflections of the particles against the planes, the directions and the orientations of the components of velocity parallel to the collision plane are maintained. In turn, the orientations of the perpendicular components of velocity are altered, while their directions remain the same as before the shocks. The elasticity of shock is defined by a coefficient of restitution of kinetic energy (Fraga Filho, 2014).

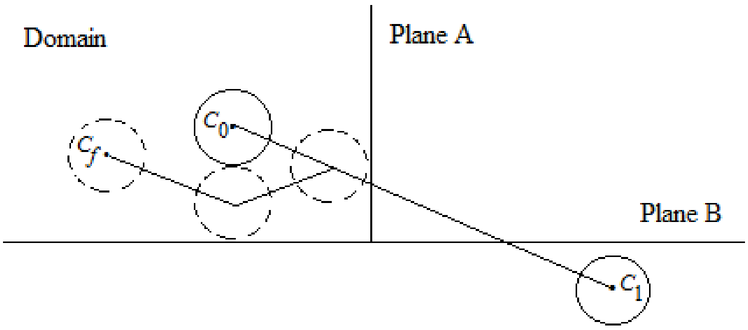

Figure 4. Collisions experienced by a particle in a time step.

An analogy to the molecular dynamics is also employed in the repulsive boundary treatment in SPH. The solid contours are areas filled with virtual particles which avoid penetration of the fluid particles. Virtual particles exert a repulsive force on the particles of the fluid, preventing them from crossing the solid outline. This force is calculated through an analogy with the Lennard-Jones molecular force. The use of a line of particles localized on the solid boundary (particles of type I) is the most applicable. Virtual particles of type II (located beyond the periphery) are also employed (Liu and Liu, 2003). Figure 5 shows the use of both types of these particles in the simulation of a solid contour.

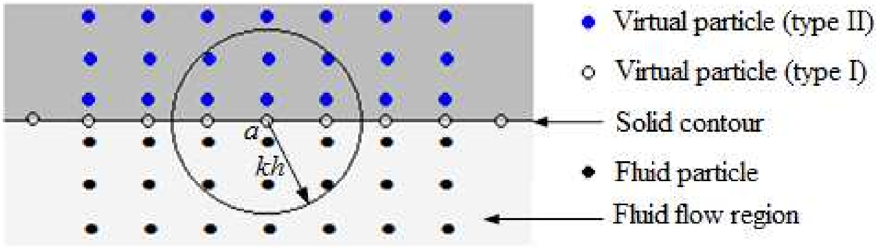

Figure 5. Schematic illustration of the solid contour region. Arrangement of the virtual particles of type I (a line on the contour) and of the virtual particles of type II (in an extended area beyond domain).

In the dynamic boundary conditions, particles located in the boundaries obey the mass conservation, momentum balance, energy conservation, and Tait equations (this latter is used for the prediction of dynamic pressures in the fluid particles). The fixed particles in the contours can be fixed or have movement (being governed by an external function imposed in the case of existence of wavemakers and gates, among others (Gomez-Gesteira et al., 2012).

The increases of the density and the particle boundary pressure occur when a fluid particle approaches. These increases cause an increase in the magnitude of the repulsion force exerted on the fluid due to the increase in the value of the term P/ρ^2 in the momentum balance equation, which results in the fluid being maintained within the domain.

Kulasegaram et al. (2004) presented the semi-analytical boundary conditions based on a variational derivation which ensures compliance with conservation laws and momentum balance. These boundary conditions took into account the kernel truncation close to the boundaries, with the renormalization being carried out, but they were effective only for certain geometries. Ferrand et al. (2012) perfected these conditions with a temporal integration scheme that allowed the renormalization for any geometry, the implementation of pressure fields close to the boundaries, and the obtaining of pressure gradients and physically correct viscous terms with a new formulation of differential operators, allowing their application in turbulent flows.

Leroy et al. (2012) effected the imposition of so-called semi-unified analytical boundary conditions on the wall (unified semi-analytical wall boundary conditions) by implementing a new Laplacian operator. The authors conducted several studies of cases in laminar (lid-driven cavity, viscous fluid flow around an infinite number of cylinders within a channel, dam breaking on a triangular edge, and flow on a water wheel) and turbulent regimes.

Fourtakas et al. (2015) implemented boundary conditions using a modified method with virtual particles on an irregular solid wall in a 2D domain based on a local point of symmetry of the contour particles. The boundary particles did not interact with the fluid particles but were used in the creation of a set of neighboring fictitious particles for each fluid particle near the walls.

In this study, the boundary treatments were performed with the use of virtual particles of type II for the hydrostatic problem and the fixed geometric planes with coefficient of restitution of energy in the collisions of particles of fluid against the boundaries in the dam breaking problem.

A flowchart of the numerical code developed in FORTRAN language is shown in Fig. 6.

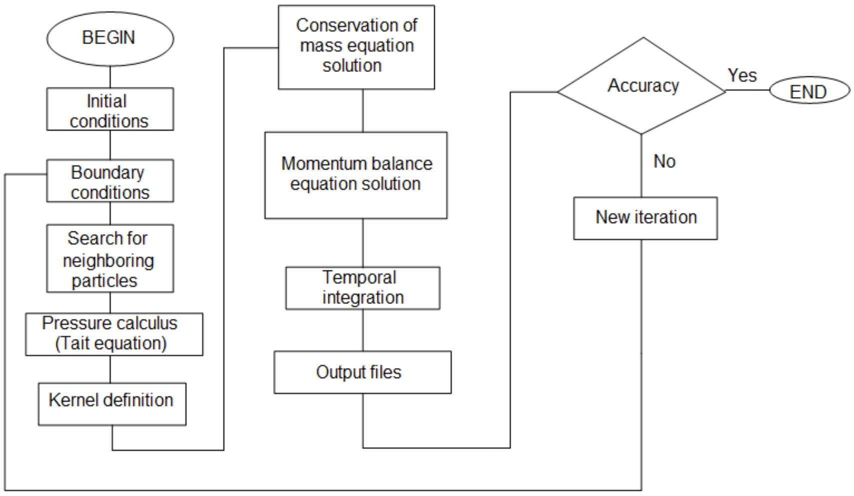

Figure 6. Flowchart showing the SPH algorithm.

4 RESULTS AND DISCUSSION

Simulations for two problems with results available in the literature or experiments were conducted: the hydrostatic case of an incompressible fluid that is uniform and isothermal inside a reservoir at rest and dam breaking.

4.1 Reservoir filled with an incompressible, uniform, and isothermal fluid at rest

This hydrostatic problem consists of a tank that is at rest, open to the atmosphere, and filled with a liquid, as shown in Fig. 7.

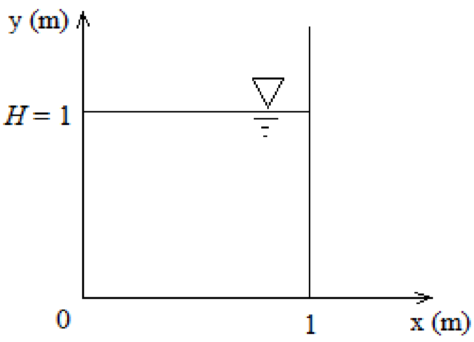

Figure 7. Open reservoir containing a uniform, incompressible, and isothermal fluid.

The physical laws of the conservation of mass and momentum balance must be obeyed in the case studied. The analysis was performed in a 2D domain. The momentum balance equation integrated in the vertical direction leads to:

$$P = P_0 + \rho g (H - y) \tag{29}$$

The origin of the referential, with a positive vertical orientation of pointing up, is fixed at the bottom of the reservoir. In the study of this hydrostatic problem, the concept of the modified pressure is applied. Combining Eqs. (6) and (29) gives Eq. (30):

$$P_{\text{mod}} = (P - P_0) - \rho g(H - \text{y}) = \rho g(H - \text{y}) - \rho g(H - \text{y}) = 0 \qquad (30)$$

As a result of Eq. (31), the modified pressure gradient is zero.

The momentum balance (Eq. (21), transcribed below), was solved.

$$\frac{D\vec{\text{v}}_a}{Dt} = -\sum_{b=1}^{n} m_b \left(\frac{P_{\text{mod}(a)}}{\rho_a^2} + \frac{P_{\text{mod}(b)}}{\rho_b^2} \right) \nabla W(X_a - X_b, h) + 2\upsilon_a \sum_{b=1}^{n} \frac{m_b}{\rho_b} (\vec{\text{v}}_a - \vec{\text{v}}_b) \frac{X_a - X_b}{\left| X_a - X_b \right|^2} . \nabla W(X_a - X_b, h)$$

The initial distribution of the particles in the domain was performed on a regular basis with 50 particles per side of the tank with dimensions of 1.00 × 1.00 m, or 2500 fluid particles in total. The number of particles within the field of influence was 21. The boundary treatment was done with the use of virtual particles of type II. Three rows and three columns of this type of particle were added on the domain side, making a total of 636 virtual particles. It was ensured that the kernel truncation would not occur (a complete domain of influence on all fluid particles was ensured). A regular distribution of them was done and, in this manner, particle inconsistency next to the border regions was avoided. The consistencies of the zeroth and first orders were assured. Figure 8 shows the initial particle distribution in the domain. The distribution of hydrostatic pressure on the fluid particles is shown in Fig. 9.

The modified pressures for all particles (fluid and virtual) at rest were initialized to zero. The time step employed was 1.00×10^{-4} s and the criterion for the convergence of Courant-Friedrichs-Lewy (1967) was obeyed. The temporal integration of the positions and velocities was done by the Euler method (Runge-Kutta first-order method).

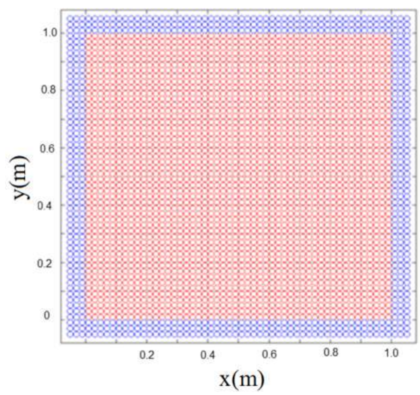

Figure 8. Initial distribution of fluid particles (red) and virtual particles (blue). The latter are in an expanded region of the domain.

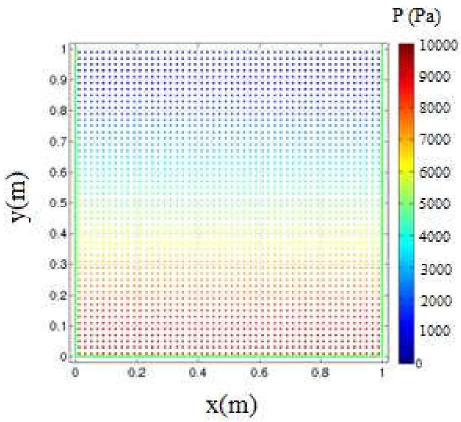

Figure 9. Hydrostatic pressure field for fluid particles.
The green line represents the walls of the reservoir.

After the solution of Eq. (22) and updating of the positions and velocities of the particles by the temporal integration in each numerical iteration, it was found that they were unchanged, maintaining hydrostatic equilibrium. Thus, the modified pressure field was maintained with a null value at the beginning of each new iteration so that the particles would remain at rest.

In the approximations to a function and its derivatives taken by the SPH method there are errors (Fraga Filho, 2014; Vaughan, 2008). When the SPH was applied without the use of modified pressure to the obtaining of approximations for the pressure and viscosity forces, terms which were present in the momentum balance equation and which were added to the gravitational force, it caused small mistakes to appear. Despite the small orders of magnitude of these errors, they spread and increased during the numerical simulation. This resulted in the appearance of particle movement, as shown in the recent studies by Vorobyev (2013), Goffin et al. (2014), Korzilius et al. (2014), and Fourtakas et al. (2015). By using the modified pressure, the sum of the gravitational force and the terms approximated by the SPH for surface forces has been avoided. Thus, the errors have been eliminated and a consistent solution to the physical problem has been obtained. The coincidence between the initial positions of the particles and the positions obtained by SPH at time 5.00 s was verified, as shown in Fig. 10.

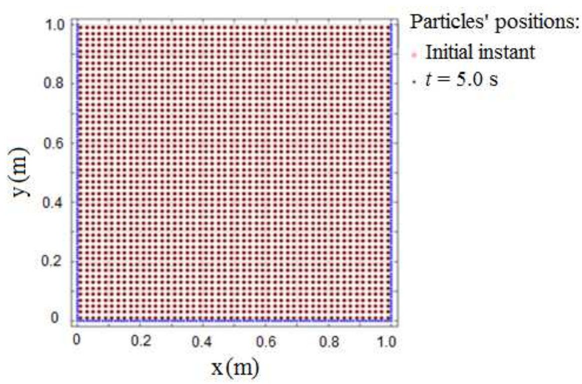

Figure 10. Coincidence between the initial positions of the particles (red circles) and their positions at time instant 5.00 s (black dots). The blue line represents the reservoir walls

4.2 Dam Breaking

In the modelling of the dam breaking, obedience to the laws of mass conservation and momentum balance was guaranteed. Numerical simulations were performed for two different heights of dammed water (H), and the results were compared to the results of experiments conducted by Cruchaga et al. (2007). The 2D computational domains simulated were: (1) a square area with height and width of 0,114 m, discretized by 1296 fluid particles, with lateral distances between their centres of mass of 3.26 mm; (2) a rectangular area with a height of 0.228 m and width of 0.114 m, discretized by 2556 fluid particles, with lateral distances between their centres of mass of 3.26 mm. The experimental apparatus is schematically shown in Fig. 11.

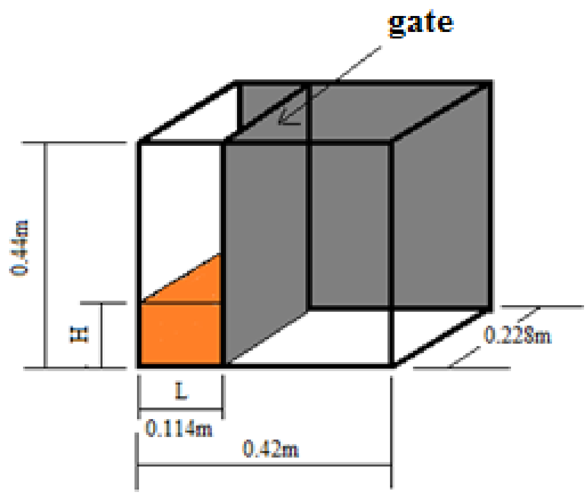

Figure 11. Experimental apparatus used in the dam breaking experiments.

The parameters used in the simulations, presented in Fraga Filho (2014), were: mathematical modelling of laminar viscous stress, estimation of the dynamic pressure field with the use of the Tait equation (term B with the value of 0.85×10^5 Pa), variation of the support radius, use of the CSPM method for correcting density and pressure gradients near the contours, boundary treatment with the use of fixed planes (against which there were totally elastic particle collisions), temporal integration by the Euler method, and a time step of 1.00×10^{-5} s. The simulations were run for a physical time of 0.50 s (50000 numerical iterations). For both geometries simulated, the artificial viscosity was implemented (Fraga Filho, 2014). The coefficient α_π received the values 0.20 and 0.30, and β_π received the value 0.00. The sound velocity in the fluid was 62.60 m/s. The free surface particles were marked and the constant pressure condition (zero) was applied first and renewed in every numerical iteration. Figure 12 presents the 2D computational domains simulated and the initial distribution of the particles.

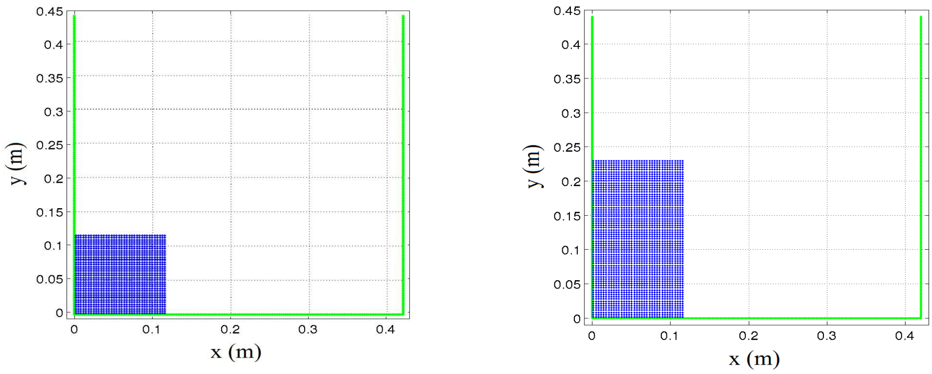

(a) (b)

Figure 12. The 2D computational domains simulated and the initial distribution of particles.

Figures 13 to 15 show the experimental and numerical results for both simulated domains.

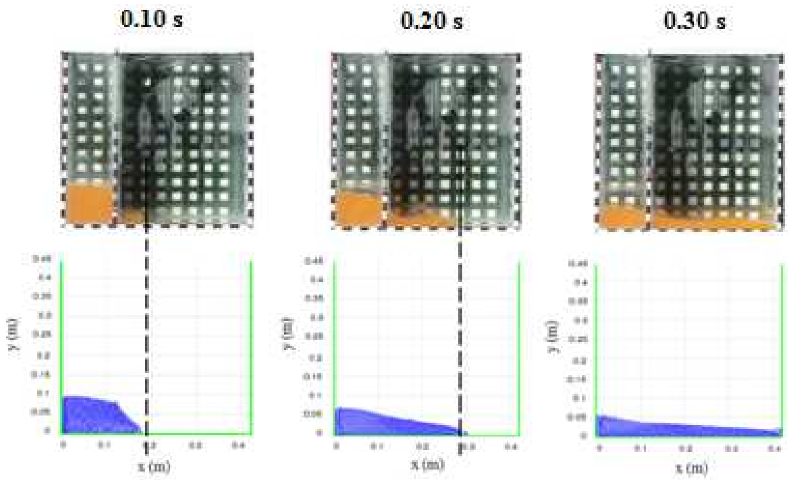

Figure 13. Experimental and numerical results for the first simulated geometry, with the implementation of artificial viscosity (α_π = 0.20).

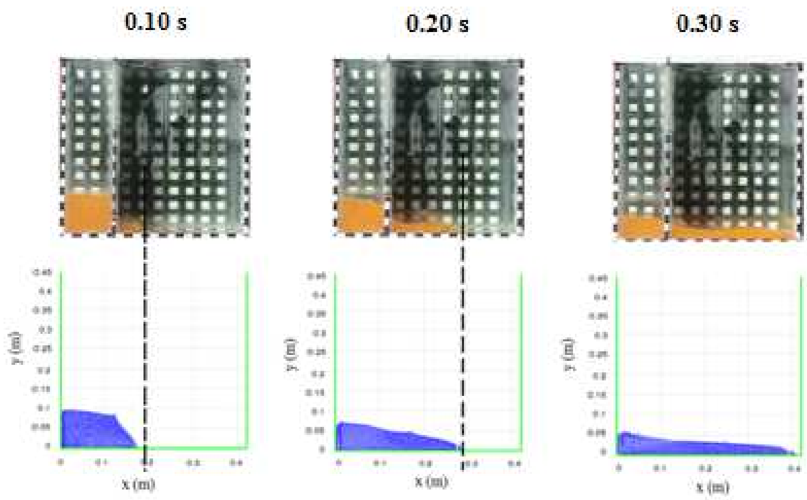

Figure 14. Experimental and numerical results for the first simulated geometry, with the implementation of artificial viscosity (α_π = 0.30).

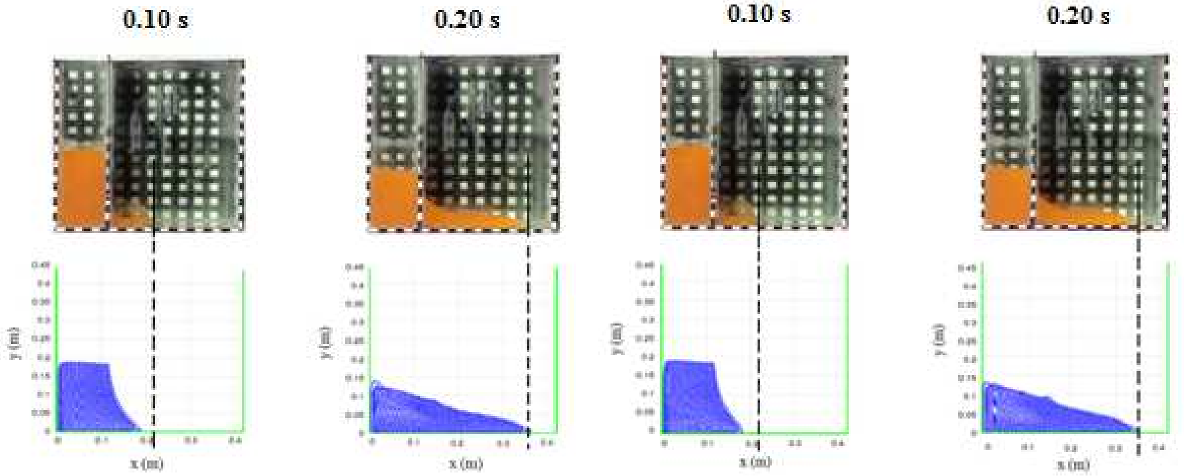

(a) (b)

Figure 15. Experimental and numerical results for the second simulated geometry, with the implementation of artificial viscosity. (a) α_π = 0.20; (b) α_π = 0.30.

Table 1 shows the percentage differences between the abscissas of the wave fronts obtained by SPH and experimentally, calculated using the expression:

$$\Delta x_p = \frac{(x_{exp} - x_{SPH})}{x_{exp}} 100 \tag{31}$$

where x_{exp} and x_{SPH} are the abscissas of the wave fronts obtained by experiments and SPH, respectively, and Δx_p is the percentage difference between the abscissas of the wave fronts.

Table 1. Percentage differences between abscissas of wave fronts (comparison between experimental and numerical results)

First Domain Simulated					Second Domain Simulated				
α_π	t (s)	x_{exp} (m)	x_{SPH} (m)	Δx_p (%)	α_π	t (s)	x_{exp} (m)	x_{SPH} (m)	Δx_p (%)
0.20	0.10	19.00	18.07	4.89	0.20	0.10	22.00	19.00	13.64
	0.20	29.00	30.28	–4.41		0.20	36.00	37.00	–2.78
0.30	0.10	19.00	17.58	7.47	0.30	0.10	22.00	18.07	17.86
	0.20	29.00	28.70	1.03		0.20	36.00	35.16	2.33

From the analysis of Table 1, the largest differences between the positions of wave fronts are seen in the early stages of dam breaking (7.47% in the first geometry and 17.86% in the second), when the coefficient α_π received the value 0.20. With the progress of time, the differences decreased, as shown at time 0.20 s. The smaller differences between wave fronts (1.03% in the first geometry and 2.33% in the second) occurred when the coefficient α_π with the value 0.30 was used.

5 CONCLUSION

The implementation of the modified pressure concept, regular distribution of particles in the domain, and boundary treatment with the use of virtual particles of type II (in an extended area of the domain, ensuring no kernel truncation led to obtaining a numerical solution in agreement with the analytical solution to the uniform hydrostatic problem of viscous and incompressible fluid at rest within a reservoir. This hydrostatic problem had not yet been satisfactorily solved with the use of the SPH method. It was found that there was no change in the positions of the fluid particles throughout the simulation time, with the complete exclusion of any oscillatory movement seen in previous studies, even after the steady state was reached.

The dam breaking case study was performed during the time before the first collision of the fluid against the wall of the reservoir. In the boundary treatment, fixed geometric planes were used as the walls, against which the particles were reflected elastically at the collision moment together with restoration of consistency of the density and of the pressure gradients (by application of the CSPM method) along with the addition of the term related to the artificial viscosity in the mathematical modelling for the laminar viscous forces acting on the fluid. The numerical results were consistent with the results of the experiments conducted by Cruchaga et al. (2007).

REFERENCES

Batchelor, G.K., 2000. *An Introduction to Fluid Dynamics*. Cambridge University Press, 3rd edition.

Chen, J.K., Beraun, J.E., & Carney, T.C., 1999. A corrective smoothed particle method for boundary value problems in heat conduction. *International Journal for Numerical Methods in Engineering*, vol. 46, pp. 231–252.

Courant, R., Friedrichs, K., & Lewy, H., 1967. On the partial difference equations of mathematical physics. *IBM Journal*, vol. 11, pp. 215–234.

Cruchaga, M.A., Celentano, D.J., & Tezduyar T.E., 2007. Collapse of a liquid column: numerical simulation and experimental validation. *Computational Mechanics*, vol. 39, p. 453-476.

Ferrand, M., Laurence, D.R., Rogers, B.D., Violeau, D., & Kassiotis, C., 2012. Unified semi-analytical wall boundary conditions for inviscid, laminar or turbulent flows in the meshless SPH method. *International Journal for Numerical Methods in Fluids,* vol. 71, n. 4, pp. 446–472.

Fourtakas, G., Vacondio, R., & Rogers, B.D., 2015. On the approximate zeroth and first-order consistency in the presence of 2-D irregular boundaries in SPH obtained by the virtual boundary particle methods. *International Journal Numerical Methods in Fluids,* published online in Wiley Online Library (wileyonlinelibrary.com).

Fraga Filho, C.A.D., 2014. Estudo da Fase Gravitacional-inercial do Espalhamento de Óleo em Mar Calmo empregando o Método Lagrangiano de Partículas Smoothed Particle Hydrodynamics. PhD Thesis, UFES, Brazil.
<http://cfd.mace.manchester.ac.uk/sph/SPH_PhDs/2014/Carlos_Alberto_DUTRA_FRAGA_FILHO_PhD_Thesis_2014.pdf>

Gingold, R.A., & Monaghan, J.J. 1977. Smoothed particle hydrodynamics: theory and application to non-spherical stars. *Monthly Notices of the Royal Astronomical Society*, vol. 181, pp. 375–389.

Goffin, L., Erpicum, S., Dewals, B.J., Pirotton, M., & Archambeau, P., 2014. Validation of a SPH model for free surface flows. Proc. 3rd SimHYDRO Conference, pp. 11–13, Nice, France.

Gomez-Gesteira, M., Rogers, B.D., Crespo, A.J.C., Dalrymple, R.A., & Narayanaswamy, M., 2010. User Guide for SPHysics Code.
<https://wiki.manchester.ac.uk/sphysics/images/SPHysics v2.2.000 GUIDE.pdf>

Gomez-Gesteira, M., Crespo, A.J.C., Rogers, B.D., Dalrymple, R.A., Dominguez, J.M., & Barreiro, A., 2012. SPHysics development of a free-surface fluid solver. Part 2: Efficiency and test cases. *Computers & Geosciences*, vol. 48, pp. 300–307.

Kelager, M., 2006. Lagrangian Fluid Dynamics Using Smoothed Particle Hydrodynamics. Department of Computer Science, University of Copenhagen.
< http://glowinggoo.com/sph/bin/kelager.06.pdf>

Korzilius, S.P., Kruisbrink, A.C.H., & Schilders, W.H.A., 2014. Momentum conserving methods that reduce particle clustering in SPH. CASA-Report 14-15, Eindhoven University of Technology.

Kulasegaram, S., Bonet, J., Lewis, R., & Profit, M., 2004. A variational formulation based contact algorithm for rigid boundaries in two-dimensional SPH applications. *Computational Mechanics*, vol. 33, n. 4, pp. 316–325.

Leroy, A., Violeau, D., Ferrand, M., & Kassiotis, C., 2014. Unified semi-analytical wall boundary conditions applied to 2-D incompressible SPH. *Journal of Computational Physics*, vol. 261, pp. 106–129.

Liu, G.R., & Liu, M.B., 2003. *Smoothed Particle Hydrodynamics: a Meshfree Particle Method*. World Scientific, Singapore.

Liu, M.B., & Liu, G.R., 2010. Smoothed Particle Hydrodynamics (SPH): an overview and recent developments. *Arch. Comput. Methods Eng.*, vol. 17, pp. 25–76.

Lucy, L.B., 1977. Numerical approach to testing the fission hypothesis. *Astronomical Journal*, vol. 82, pp. 1013–1024.

Monaghan, J.J., 1992. Smoothed particle hydrodynamics. *Annual Review of Astronomy and Astrophysics*, vol. 30, pp. 543–574.

Morris J.P., Fox, P.J. and Zhu, Y., 1997. Modeling Low Reynolds Number Incompressible Flows Using SPH. *Journal of Computational Physics*, Vol. 136, p. 214-226.

Nobrega, T.H.C., 2007. Sistema de Partículas para Modelagem e Simulação Interativa de Fluidos. End of Course Work in Computer Science. Federal University of Santa Catarina, Brazil.

Vaughan G.L., Healy, T.R., Bryan, K.R., Sneyd A.D., & Gorman, R. M., 2008. Completeness, conservation and error in SPH for fluids. *International Journal for Numerical Methods in Fluids*, vol. 56, pp. 37–62.

Vorobyev, A., 2013. *A Smoothed Particle Hydrodynamics Method for the Simulation of Centralized Sloshing Experiments*. KIT Scientific Publishing, Germany.